An Initial Validation of the NASA TROPICS Pathfinder Microwave Radiometer Observations

Amelia Gagnon *Student Member, IEEE*, Samantha N. Hasler, Juliana Chew, William Blackwell *Fellow, IEEE*, R. Vincent Leslie *Senior Member, IEEE*, Michael DiLiberto, Kerri Cahoy *Member, IEEE*

***Abstract*—The NASA Time-Resolved Observations of Precipitation structure and storm Intensity with a Constellation of Smallsats (TROPICS) Pathfinder CubeSat was placed into a sun-synchronous orbit by a SpaceX Falcon 9 launch vehicle during the June 30, 2021 Transporter-2 rideshare mission. The Pathfinder satellite carries a microwave radiometer with twelve channels (spanning 90 to 205 GHz) that are sensitive to the precipitation, humidity, and temperature structure of Earth's atmosphere. In this work, we compare the TROPICS Pathfinder calibrated brightness temperatures (radiances) to collocated European Centre for Medium-Range Weather Forecast's Reanalysis v5 (ERA5) data and radiative transfer simulations of Earth's atmosphere using the Community Radiative Transfer Model (CRTM). To minimize errors due to radiative transfer uncertainties, we compare TROPICS Pathfinder L1B data from October 2021 with simulated brightness temperature values from the CRTM for observations that are filtered for points near-nadir, over-ocean, free of clouds, and within latitudes from 40° N to 40° S. We also step through each of the filtering steps individually, to reduce the modeling errors in our comparison. Our results indicate excellent agreement with the simulated brightness temperatures, attaining less than 1 K mean difference between Pathfinder observed radiances and the CRTM simulated radiances for all channels, which is within the 1 K mission requirement.**

***Index Terms*—Remote sensing, microwave radiometry, calibration, Earth, atmospheric measurements**

I. Introduction

THE NASA Time-Resolved Observations of Precipitation structure and storm Intensity with a Constellation of Smallsats (TROPICS) Pathfinder satellite (Pathfinder) is the Engineering Qualification Unit and a precursor spacecraft to the full TROPICS constellation. TROPICS Pathfinder was launched in June 2021 to checkout and optimize all TROPICS mission elements prior to the launch of the constellation. The full constellation of four 3-Unit (3U) CubeSats was placed into orbit on May 8, 2023 and May 26, 2023 New Zealand Standard Time. The TROPICS mission is now providing observations of Earth's atmospheric temperature and humidity structure over all tropical latitudes and pressure levels, from approximately 1000 hPa to 50 hPa, or from Earth's surface to ∼20 km in altitude [1]. Additionally, the constellation is collecting observations of the Earth's atmosphere at high temporal resolution (around 60-minute median revisit rate), which is critical for monitoring the rapidly-evolving features of tropical cyclones [2].

Manuscript received June 24, 2024; This work was funded by NASA grant NNL16AA57I. A. Gagnon and S. N. Hasler would also like to acknowledge support from the MathWorks Fellowship. *(Amelia Gagnon and Samantha N. Hasler are co-first authors.) (Corresponding author: Amelia Gagnon.)*

The Pathfinder satellite collected observations from August 2021 to December 2023. These observations also include precipitation [3], [4] and atmospheric sounding [5] information, with the ultimate goal of using these data to improve tropical cyclone forecasting.

Pathfinder was the first CubeSat sounder to make global observations of the Earth's atmosphere, and it did so on an extended timescale. The Pathfinder Level 1B (L1B) data was successfully downlinked from Pathfinder with data availability hosted on the TROPICS Data Processing Center [6]. An example of global observations produced by Pathfinder is shown in Figure 1. Pathfinder stopped producing science data in mid-December 2023 and was decommissioned for de-orbit in May 2024. It substantially exceeded the TROPICS design lifetime of 20 months, and did so after withstanding the rigors of harsh pre-launch qualification testing beyond the nominal acceptance level testing undergone by the main TROPICS constellation.

For CubeSat radiometers to be viable as a suitable low-cost alternative to larger systems, calibration must be consistent during the mission lifetime and also produce highly accurate observations. To address this critical need, this work presents an initial analysis of a subset of data from Pathfinder to provide an assessment of calibration accuracy as compared simulated brightness temperatures and serves as an introduction to our validation process, which will be applicable to the full TROPICS constellation. We define validation in this context as it is defined in [7], where observed brightness temperatures are compared with simulated radiances. We aim to determine the quality of the data product from Pathfinder as compared to other sources, such as European Centre for Medium-Range Weather Forecast's (ECMWF) Reanalysis v5 (ERA5) dataset with the Community Radiative Transfer Model (CRTM).

In this work, we introduce our method to validate on-orbit data collected by the TROPICS satellites and run the routine on observations collected by Pathfinder in October 2021. The goal of our data validation is to ensure that Pathfinder's microwave radiometer meets mission precision and accuracy requirements by comparing observational conditions that are the same as what we can robustly obtain from model output. This validation process is a separate process from the operational data release checks, which instead assess the quality of all data before public release. At the present time, calibration and validation activities for the TROPICS constellation satellites are ongoing, and a validation of the full constellation will be addressed in future work.

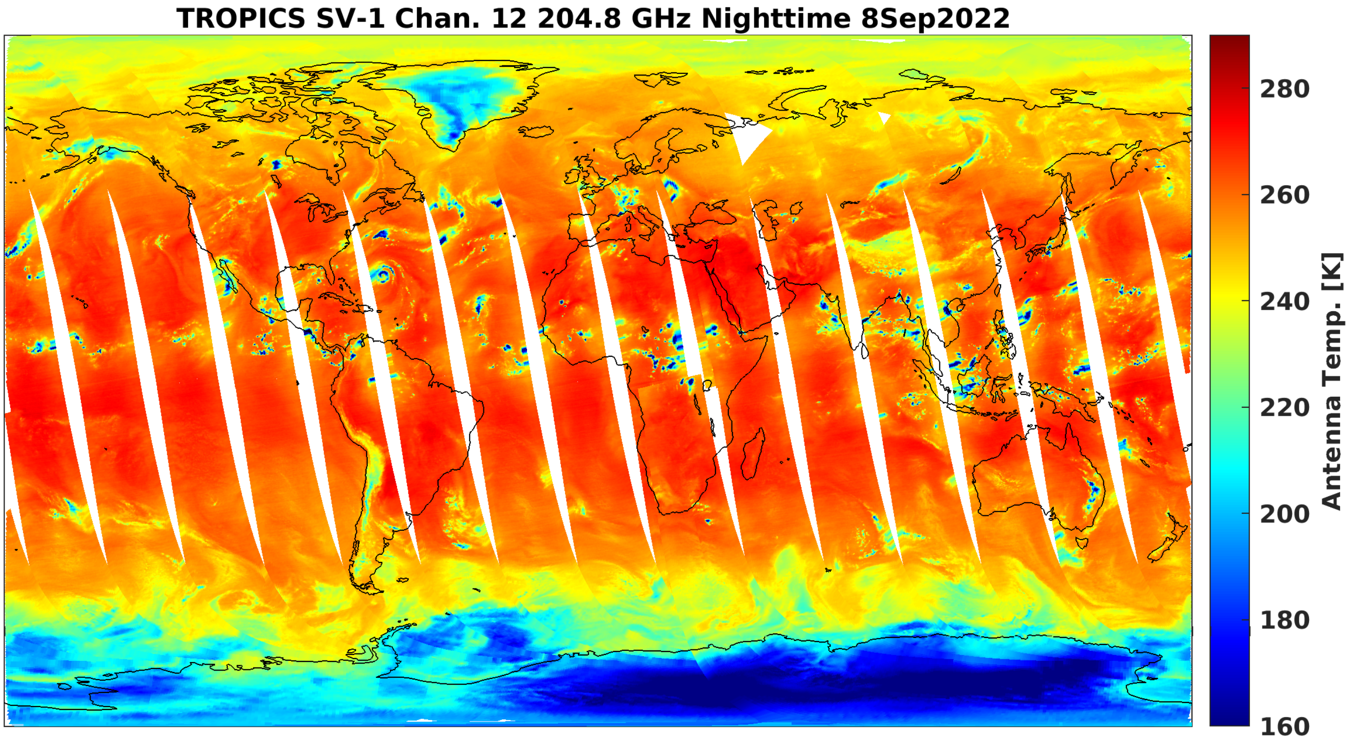

Fig. 1. Global nighttime observations from TROPICS Pathfinder in Channel 12 from half of the day on September 8, 2022 in a sun-synchronous orbit. Hurricane Earl is visible in the western portion of the Atlantic Ocean. The color bar displays the radiometric antenna temperature in Kelvins.

A. TROPICS Mission Overview

Four 3U CubeSats comprise the TROPICS constellation mission: TROPICS-03, -05, -06 and -07. The constellation was launched in pairs, 05/06 and 03/07, aboard a Rocket Lab Electron launch vehicle on May 8, 2023 and May 26, 2023, respectively. Each pair orbits the Earth in separate low-Earth orbital planes with an inclination of 33° and an initial altitude of 550 km. The two orbital planes were initially separated by 180° in Right Ascension of the Ascending Node (RAAN). Within each plane, the satellite pairs will slowly and persistently change spacing with minimal impact on revisit rate [1].

TROPICS Pathfinder, the precursor CubeSat to the full constellation and designated TROPICS-01, was launched on June 30, 2021 on the SpaceX Transporter 2 mission to a sun-synchronous orbit with an altitude of approximately 520 km and local time of the ascending node of approximately 02:00 AM. Pathfinder carries an identical payload to the other TROPICS satellites, and is the focus of this work.

The TROPICS satellites are designed to provide measurements of tropical cyclones at tropical latitudes (approximately 40° N to 40° S) using a passive microwave radiometer [8]. The measurements provide information on troposphere thermodynamics and the precipitation structure of tropical cyclones to advance predictions of storm track and intensity [9]. The mission requirements include calibration accuracy within 1 K for four of the twelve channels (Bands 3 and 4), within 1.5 K for seven of the twelve channels (Band 2), and within 2 K for one channel (Band 1) [1]. All channels and analysis bands are listed in Table I.

The spacecraft bus for each TROPICS unit is based on the Blue Canyon Technologies XB3, a 3U-sized CubeSat. Additional XB3 specifications available online [10]. The scientific objectives for the mission can be found in Section I-B. The ultimate goal of the TROPICS mission is to provide high-value science investigations of tropical cyclones at higher temporal resolution compared to other on-orbit passive microwave radiometers (e.g., Global Precipitation Measurement Microwave Imager [11]) [1].

B. Science Objectives

The mission's overarching goal is to provide nearly all-weather observations of the troposphere's 3-D temperature and humidity structures to investigate the lifecycles of tropical cyclones. The first mission objective is to determine the relationship between precipitation structure, upper-level warm-core evolution, and storm intensity changes of tropical cyclones. In addition, the mission aims to relate the evolution of tropical cyclone precipitation structure and storm intensification to environmental humidity fields. The third objective is to determine the impact of the TROPICS constellation's more frequent observations on the numerical and statistical forecasts of tropical cyclones [1].

C. TROPICS Payload

Pathfinder and all other CubeSats in the TROPICS constellation have a passive microwave radiometer payload that

TABLE I
TROPICS CHANNELS WITH FREQUENCIES IN GHZ, BEAMWIDTH IN THE DOWN-TRACK AND CROSS-TRACK DIRECTION IN DEGREES, NADIR SCAN SPOT SIZES IN KM AND CORRESPONDING ANALYSIS BANDS

Channel	Frequency (GHz)	Beamwidth (Down°/Cross°)	Cross Track (km)	Along Track (km)	Analysis Band
1	91.655 ± 1.4	3.0/3.17	30.4	28.8	Band 1
2	114.50	2.4/2.62	25.2	23	Band 2
3	115.95	2.4/2.62	25.2	23	Band 2
4	116.65	2.4/2.62	25.2	23	Band 2
5	117.25	2.4/2.62	25.2	23	Band 2
6	117.80	2.4/2.62	25.2	23	Band 2
7	118.24	2.4/2.62	25.2	23	Band 2
8	118.58	2.4/2.62	25.2	23	Band 2
9	184.41	1.5/1.87	17.9	14.4	Band 3
10	186.51	1.5/1.87	17.9	14.4	Band 3
11	190.31	1.5/1.87	17.9	14.4	Band 3
12	204.80	1.4/1.83	17.3	13.4	Band 4

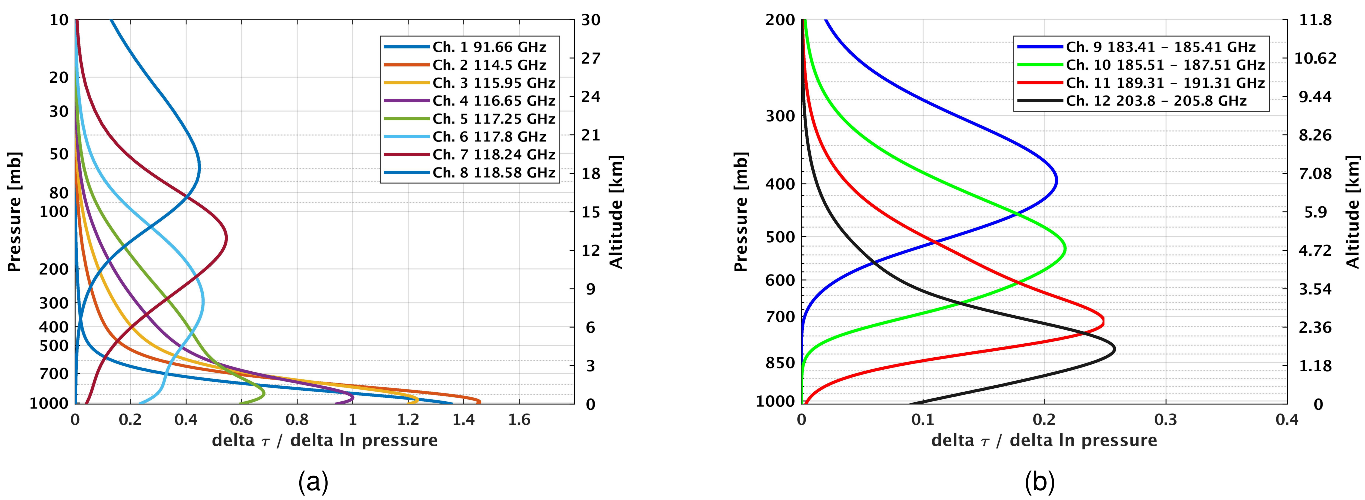

Fig. 2. Weighting functions for each of the 12 channels on the TROPICS microwave radiometer. Functions were calculated with an angle of 0° incidence (nadir) through a standard tropical atmosphere and a perfectly emissive surface. Figure 2a displays weighting functions for channels 1–8, corresponding with analysis bands 1 and 2 and sensitive to temperature. Figure 2b displays channels 9–12, corresponding with analysis bands 3 and 4 and sensitive to water vapor. In (a) and (b), τ stands for the atmospheric transmittance. Image credit: [1]

was developed at the Massachusetts Institute of Technology (MIT) Lincoln Laboratory. While all satellites in the main constellation orbit at an inclination of approximately 33°, the orbital design of the TROPICS mission has two pairs of satellites operating in their own orbital plane. In contrast, Pathfinder observed from a nearly-polar (sun-synchronous) orbit.

The payload consists of a 12-channel passive microwave radiometer that operates at 100% duty cycle and measures spectral radiance over the cross-track direction of the satellite. As shown in Table I, seven of the twelve channels provide measurements near 118.75 GHz, three channels near 183 GHz, one channel near 90 GHz, and one channel near 205 GHz [1].

The observation channels on the TROPICS microwave radiometers were chosen to specifically probe various structures and altitudes in Earth's atmosphere, from the surface up into the stratosphere [1]. Figure 2 (from [1]) displays the weighting functions of the TROPICS payload to illustrate the atmospheric regions to which each channel is sensitive. The transmittance (τ) in Figure 2 is the fraction of transmitted electromagnetic radiation. Channel 1 (around 90 GHz) provides imagery and information about the precipitation structure when combined with other channels. Channels 2 through 8 probe the region near the oxygen absorption line near 118 GHz and can provide temperature information. Channels 9 through 11 probe the 183 GHz region near the atmosphere's water vapor absorption, which provides moisture information. Channel 12 is centered near 205 GHz to capture cloud-ice particles.

The payload operates by spinning continuously at a rate of 30 revolutions per minute (RPM) perpendicular to the direction of CubeSat travel, also called the "cross-track" direction. [12]. The scanning requirements are described in detail in [12]. The pointing (geolocation) accuracy for Pathfinder is illustrated in Figure 3 and is generally a very small fraction of the footprint diameter ($< 1/20$) for all channels.

The thermal variation of the radiometer over the course of an orbit is relatively small ($\sim$10° C). The orbital variation of Pathfinder modulates a peak-to-peak thermal variation between 7° to 9° C over a year. The calibration algorithm for each satellite can operate through these variations with negligible errors because of periodic absolute calibration, see Section

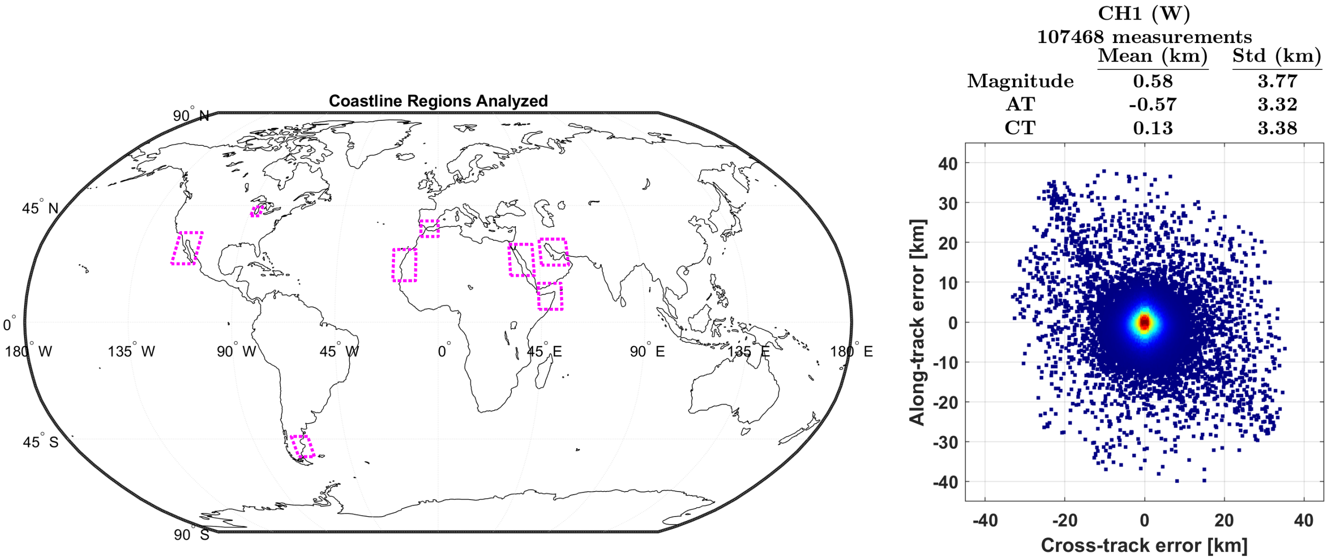

Fig. 3. Pathfinder geolocation performance. Left: regions where geolocation performance is measured for Pathfinder are highlighted by the dashed boxes. Right: the measured near-nadir geolocation accuracy of Pathfinder between August 7, 2021 to July 31, 2023 is shown. The measurements include scan angles less than 24 degrees from nadir and were made using the coastline inflection method [14].

I-D. We refer the reader to [1], [12] and [13] for additional information on the TROPICS spacecraft and payload.

D. Instrument Calibration

Calibration of microwave radiometers typically involves a two-point "warm" and "cold" reference point scheme. The warm calibration point for the TROPICS payload is a weakly coupled noise diode; the cold reference point is deep space [15]–[18]. For TROPICS Pathfinder, the payload was calibrated pre-launch at MIT Lincoln Laboratory using a calibration apparatus containing three calibration targets representing Earth view, a cold reference, and a warm reference.

On-orbit, the radiometer calibration on Pathfinder and now the TROPICS constellation happens once per payload scan, which is every two seconds. The radiometer is calibrated with two steps. First, noise is injected using the weakly coupled noise diode into the front end of the radiometer while it is viewing the cosmic background. The cold calibration is then performed by measuring the cosmic background with the noise diode off [19].

E. Comparison to Other Microwave Instruments

The TROPICS CubeSat mission was designed to provide fast revisit rates and accomplish the same objectives as larger satellites with microwave sounders, but with a reduction in cost compared to larger satellites. Currently operational passive microwave radiometer atmospheric sounders on programs with observing frequencies overlapping TROPICS (see Table I) include the Advanced Technology Microwave Sounder (ATMS) series, the Advanced Microwave Sounding Unit -A and -B, the Microwave Humidity Sounder (European Organisation for the Exploitation of Meteorological Satellites), the Imaging/Sounding Microwave Radiometer series, the Micro-Wave Radiation Imager series, and the Micro-Wave Humidity Sounder series (China Meteorological Administration) instruments, among others [20]. However, no singular instrument contains frequencies that overlap with all four TROPICS bands.

Revisit times for each of these instruments are once or maximum twice per day and with coverage globally or semi-globally. These lower revisit times highlight the observational gap of having rapid revisit capabilities for developing weather systems. Observation footprint sizes on large microwave radiometers range from only a few kilometers [21] to 16 km [22], comparable to the TROPICS scan-spot sizes at nadir. In future work, these on-orbit radiometers may be suitable candidates for performing cross-comparison between on-orbit satellites with the TROPICS microwave radiometer observations. We expand on the potential for cross-comparison in Section V.

F. Validation of Microwave Radiometers

To perform data validation for Pathfinder, we compare the on-orbit L1B radiance data product (version 1.0) [6] to another data source to determine the overall quality of the instrument data product. We develop a validation scheme similar to those used for the Micro-sized Microwave Atmospheric Satellite-2A (MicroMAS-2A) and other on-orbit passive microwave radiometer missions [7], [23]. We compare TROPICS Pathfinder radiances to simulated radiances generated by the Community Radiative Transfer Model (CRTM) [24], using ERA5 reanalysis data as the model input. More information about the datasets and methods used in the validation scheme can be found in Section II and Table III.

For CubeSat radiometers to be viable as a suitable low-cost alternative to larger systems, calibration must be consistent during the mission lifetime and the instrument must have highly accurate observations. In this initial validation of the Pathfinder data, we find that all twelve channels of the

This article has been accepted for publication in IEEE Journal of Selected Topics in Applied Earth Observations and Remote Sensing. This is the author's version which has not been fully e
content may change prior to final publication. Citation information: DOI 10.1109/JSTARS.2024.3518541

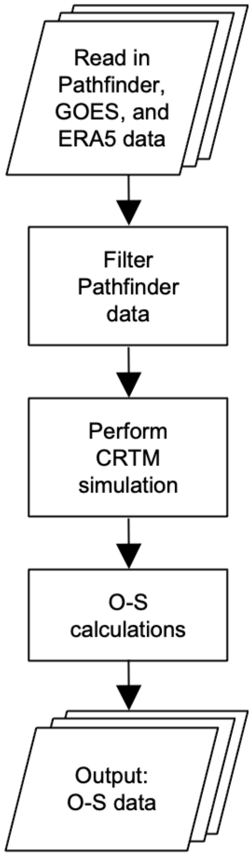

Fig. 4. Data validation methodology for the TROPICS Pathfinder microwave radiometer data. O-S refers to the Observation minus Simulated calculation, which compares the observed brightness temperatures collected on-orbit (O) to simulated brightness temperatures using ERA5 reanalysis data (S) to determine quality of instrument performance. Details for the data filtering scheme are shown in Figure 5.

TROPICS microwave radiometer have mean biases of <0.5 K and standard deviations ≤ 3 K when compared with simulated brightness temperatures during the month of October 2021 (see Section III).

The remainder of this paper is organized as follows: In Section II, we describe in detail the architecture of the validation methodology and the data inputs. We apply our methodology to a subset of data from the Pathfinder satellite and describe the results in Section III. Section IV presents a discussion of our results. We summarize and describe directions for future work in Section V.

II. Validation Architecture

Figure 4 displays the overall data validation process. Pathfinder radiances are filtered to reduce radiative transfer modeling uncertainties, as described in Sections II-A and II-B. After generating the corresponding simulated radiances (also known as "simulated" and "S" hereafter) using the CRTM (see Section II-C), we calculate the difference between the Observed-Simulated (O-S) brightness temperature for each channel.

A. Data Inputs

There are three datasets that are required to perform our O-S validation: Pathfinder observations, Geostationary Operational Environmental Satellite (GOES) cloud observations, and ERA5 reanalysis data. Each of these datasets are discussed in greater detail below.

1) TROPICS Pathfinder Data: We use the L1B (version 1.0) TROPICS Pathfinder observations [6] from the month of October 2021 in the analysis presented here. October 2021 was selected based on high data availability and quality at the time of selection. Data between 00:00-23:00 UTC were used for each day. Data latency on the NASA Goddard Earth Sciences (GES) Data and Information Services Center (DISC) website is about 12 hours, but data are available with latency of approximately 60 minutes upon request. At the time of writing, Pathfinder data are now available from August 2021 to mid-December 2023, and an expanded validation to that presented here is now underway and will be described in future work. The dataset analyzed here includes information related to each observation such as latitude, longitude, time, scan angle, zenith angle, and brightness temperature. All of the information listed corresponds to the following fields given in the data: $latitude$, $longitude$, $time$, $sensor\_view\_angle$, $sensor\_zenith\_angle$, and $brightness\_temperature$, respectively. Additionally, each observation has land/sea and data quality flags.

2) GOES Cloud Observation Information: To filter out cloudy observations, we use the GOES Clear Sky Mask Product. This is a GOES Level 2 product that contains a Binary Cloud Mask (BCM) with pixels labeled as "clear" or "cloudy" [25], [26]. This dataset has a resolution of 2 km x 2 km for the Advanced Baseline Imager (ABI) bands, which is the primary weather imaging instrument aboard the current GOES satellites.

We compare GOES-16 and GOES-17 satellite data with October 2021 Pathfinder observations, to select for observations that are clear of clouds. The GOES spacecraft are in geostationary orbit and provide a full disk view of the Earth centered at 75.2° West and 137.2° West for GOES-16 and GOES-17, respectively. These views cover much of the Pacific Ocean and provide nearly full visibility of North America [27]. Views from both spacecraft combined provide us with access to cloud data for over half of the longitudinal range of the TROPICS observations. More information on how both datasets are incorporated can be found in Section II-B3.

The GOES ABI default scan mode (Scan Mode 6) takes a full disk image every 10 minutes, with approximately 30 seconds between observation files [27]. The BCM is generated using algorithms with a set of spatial, spectral, and temporal tests to discern clear versus cloudy sky [28], [29]. The initial cloud mask that is produced, which the BCM is derived from, classifies pixels into four levels: Clear, Probably Clear, Probably Cloudy, and Cloudy. The test for clear and cloudy sky is applied on a pixel-by-pixel level, resulting in a cloud or no cloud result for each pixel. The algorithm is described in detail in [28]; each threshold is set to minimize false detections for all surface types (i.e., the majority of clouds should be detected with the combination of multiple tests). [29] reports that the BCM has ~90% accuracy in detecting clouds. Clouds that are missed by the BCM include thin clouds and those with low emissivity [29]. We expect thin clouds to have little overall impact on the radiative transfer as compared to thicker clouds.

For our validation procedure, we use the latitude, longitude, binary cloud mask, data quality flag, scan angle, elevation angle, and the observation start and end times from the GOES data. The data quality flag ranges from 0-6, where points marked as 0 indicate “good quality” observations. We filter the BCM for “clear or probably clear” points where the BCM indicates clear sky (flagged as ‘0’), and then compare the geographical locations of the cloud mask points to the Pathfinder data.

3) ERA5 Reanalysis Data: To perform radiative transfer simulations of Earth’s atmosphere during a TROPICS observation, the radiative transfer model requires input for the atmospheric temperature profile and properties during the time of the observation. This work uses the ERA5 reanalysis data published by the ECMWF as the source to validate Pathfinder data against. Other options for reanalysis data include the Modern-Era Retrospective Analysis for Research and Applications, version 2 (MERRA-2) [30] and the Climate Forecast System Version 2 (CFSv2) [31]. ERA5 was chosen for this work because it has finer temporal and spatial resolution, resulting in a higher number of observation collocations with the TROPICS data.

ERA5 data has a temporal resolution of 1 hour and spatial resolution of 0.25° by 0.25° in latitude and longitude. The data ranges from Earth’s surface to a top pressure level at 0.01 hPa. Initial release ERA5 data is published within five days of measurement, with a final data release occurring within three months. The quick-release schedule and data resolution makes the ERA5 dataset ideal for use in rapid TROPICS radiance validation.

To simulate Pathfinder microwave radiometer observations, both ERA5 Pressure Levels [32] and ERA5 Hourly Surface [33] are used to get a full atmospheric profile. Specific variables used in this work from the ERA5 Pressure Levels are temperature, specific humidity, geopotential, ozone mass mixing ratio, and specific cloud liquid water content. Variables called from the ERA5 Hourly reanalysis data in this work are mean sea level pressure, surface pressure, 10 m u- and v-components of wind, sea surface temperature, ice temperature layers 1-4, and sea-ice cover.

ERA5 is known to exhibit random uncertainties due to observations, sea surface temperature, and physical model parameterizations [32], but the data have relatively low uncertainty in the parameter space that we probe in this work. While ERA5 has several known issues, most occur at altitudes higher than those probed by the TROPICS radiometric channels or occur over land [34]. ERA5 is also known to experience difficulty with detection and estimation of precipitation events [35], [36]. However, comparisons of variables from ERA5 to other reanalysis datasets indicate that ERA5 has the closest agreement to observations (e.g., for atmospheric winds or precipitation measurements) [36], [37].

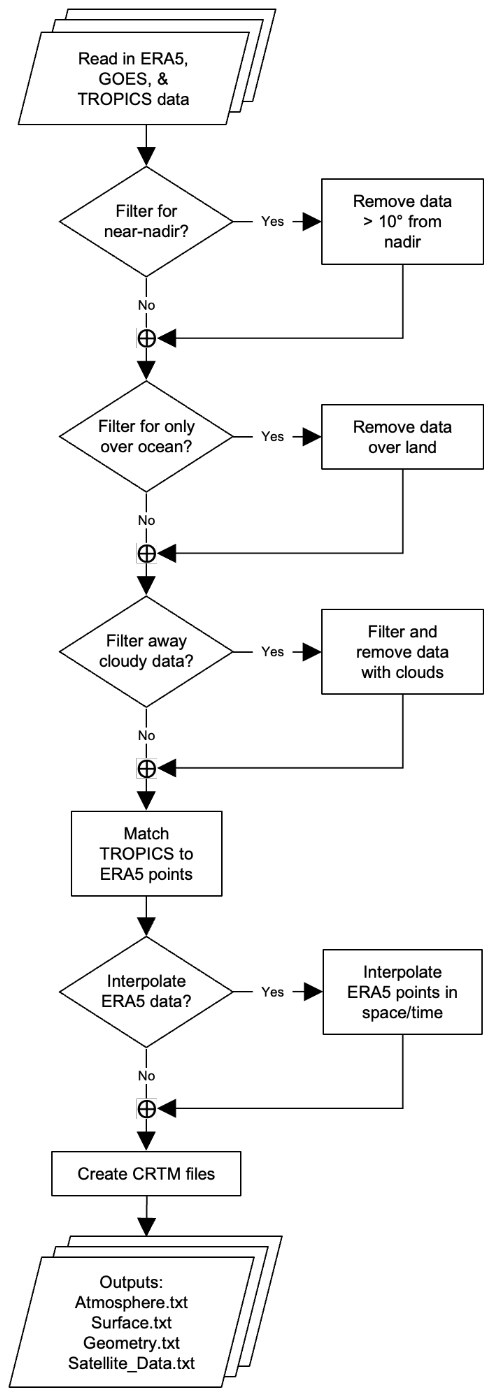

Fig. 5. Data filtering flow in the validation script. Data can be filtered as set by the user and is described in detail in Section II-B. Our filtering points are notated here as nodes labeled as “Yes”. From the beginning of the process, the first filtering step is to save only observations within a certain degree of nadir (here, we have chosen to remove points greater than 10° from nadir). Next, we filter for observations over only ocean and remove points taken over land. We then filter out the observations affected by clouds using the GOES Binary Cloud Mask. Finally, we choose to interpolate the ERA5 Reanalysis data, to find the nearest points in space and time to the TROPICS observation. The data filtering process ultimately results in the Atmosphere, Surface, and Geometry profile files required for the CRTM run and a “satellite data” file containing observed brightness temperatures.

B. Filtering TROPICS Pathfinder Data

The first step of the validation method is to filter the Pathfinder dataset for observations that are usable for O-S comparison. We use MATLAB as the data-formatting language because of its ability to handle large datasets and format data

TABLE II
STEP THAT EACH FILTER WAS ADDED DURING THE DATA PROCESSING PROCEDURE. FILTERS WERE ADDED CUMULATIVELY FOR COMPARISON. RESULTS FROM EACH STEP ARE ILLUSTRATED IN FIG. 6.

Filtering step	Filter name				Number of points per band			
	Near Nadir	Over Ocean	Cloud Free	ERA5 Interpolation	Band 1	Band 2	Band 3	Band 4
Step 1	X	–	–	–	4,387,590	4,388,045	4,383,612	4,382,226
Step 2	X	X	–	–	4,276,527	4,276,983	4,272,584	4,271,288
Step 3	X	X	X	–	160,052	205,275	318,643	336,039
Step 4	X	X	X	X	157,131	201,120	311,078	327,900

for the CRTM input. Prior to performing any data filtering, all Pathfinder data is ingested into MATLAB on a per-day basis for October of 2021. The data includes the full range of latitudes observed by Pathfinder, all observation times, both land and sea observations, and all scan angles that were observed.

For our analysis, we consider only observations within a latitude range of 40° N to 40° S, to reflect the latitudes that are observed by the full TROPICS constellation. The filtering process is outlined in Figure 5 and Table II. Table II illustrates each filtering step and which filters were applied. The number of data points that are left after each applied filter are listed in the right-hand column for each observation band. In the following sections, we build up our data filtering procedure step by step. We compare the results before and after adding each filtering step, starting with Section II-B1.

1) Filtering for Near-Nadir Data: To filter for near-nadir observations, we use the $sensor\_view\_angle$ variable provided in the TROPICS Pathfinder L1B data. This variable describes the scan angle, which is the angle between local nadir at the satellite and the line-of-sight vector to the Earth's surface. As the scan angle increases, the scan spot footprint increases in size. For instance, the nadir scan spot for TROPICS Pathfinder's W band (Channels 2-8) has a geometric mean radius of 29.6 km, whereas the scan spot at a scan angle of 60° has a geometric mean radius of 121.1 km [15]. For our O-S validation process, we set the scan angle bounds to be within $\pm 10°$ of nadir. By limiting our observations for analysis in this way, the remaining observations are measured over a similar dimensional area geographically.

2) Filtering for Over-Ocean Data: Due to the challenges involved with land surface emissivity modeling and the fact that TROPICS is a tropical cyclone mission, we filter the Pathfinder observations to include only over-ocean observations points. By doing so, we aim to reduce errors introduced in the radiative transfer modeling process and ensure our O-S calculations are well modeled by the CRTM. Modeling radiative transfer interactions with land surface components is particularly challenging due to varying physical properties that must be accounted for (e.g., soil moisture, topography, surface type, scattering properties). [38] presents a detailed evaluation of modeled emissivities over land.

The TROPICS Pathfinder L1B radiance product (version 1.0) contains the *LandFlag* variable, where values are categorized as either 0, 1, or 2, which correspond to observations of ocean, land or coastline, and undefined/poor geolocation, respectively [23]. We use this flag to filter for the points that are over the ocean in the TROPICS Pathfinder data for further analysis.

3) Filter for Cloud-Free Data: We use cloud-free observations from TROPICS to minimize discrepancies due to cloud modeling errors. The accuracy of radiative transfer modeling with clouds generally decreases with increasing frequency. This correlation is due to a variety of factors, which include cloud particle properties, cloud types, ozone quantities, and water vapor continuum absorption effects [39], [40]. We determine whether an observation has clouds by using the GOES-16 and GOES-17 BCMs. More information about the GOES data source can be found in Section II-A2. Notably, the observation regions for GOES-16 and GOES-17 overlap. We choose which GOES cloud observation source to use for each TROPICS observation with the following criteria, in order of importance:

1) Data Quality
2) Distance from Pathfinder observation to the GOES BCM pixels

By using the above criterion in that order, we account for the GOES-17 data quality adjustment that is occasionally needed due to satellite heating [41] and favor observations that are closer to their respective GOES instrument nadir. This data quality determination is important for us to ensure that the GOES cloud observation is subject to the least possible amount of parallax in measurement. That is to say, the clouds are being measured as close to their location on-sky as possible. We use the sum of the provided GOES scan and elevation angle magnitudes as a proxy for a location's distance to GOES nadir. In doing so, greater angle sums equate to greater distances from GOES nadir.

4) Using Custom Scan Spots: The TROPICS microwave radiometer has three frequency bands for observation that can be separated further into four analysis bands, which are shown in Table I. The F Band is Band 1 (which includes Channel 1), the W Band includes Band 2 (which includes Channels 2-8), and the G Band includes both Bands 3 and 4 (Channels 9-11 and Channel 12 respectively). The beam width of the observation is dependent on the band (or frequency), so the observation scan spots projected onto the Earth will have band-specific sizes. Table I displays the corresponding scan sizes for each band for the nadir scan spot. Dimensions for all scan spots are included in [15], as they vary by frequency and distance from nadir. Additional information regarding scan spot size variability in the cross-track direction for different bands can be found in [1].

We account for the variation in scan spot sizes in our validation by approximating the area of the projected scan ellipse defined by the cross-track and down-track dimensions.

TABLE III
INPUT VALUES SET IN THE CRTM ATMOSPHERE AND SURFACE INPUT FILES. SURFACE VARIABLE VALUES ARE LISTED WITH THEIR NPOESS CLASSIFICATION SCHEMES, AS GIVEN IN THE SECTION 4.6 OF THE CRTM USER'S GUIDE [42].)

Input file	Variable name	Value
Atmosphere	Climatology	US_STANDARD_ATMOSPHERE
	Absorber_ID	H2O_ID, O3_ID
	Absorber_Units	MASS_MIXING_RATIO_UNITS, VOLUME_MIXING_RATIO_UNITS
Surface	tundra_surface_type	10
	scrub_surface_type	7
	coarse_soil_type	1
	groundcover_vegetation_type	7
	bare_soil_vegetation_type	11
	sea_water_type	1
	fresh_snow_type	2
	fresh_ice_type	1

To simplify the filtering process, we utilize a square area whose side length is the smaller dimension. Accounting for the scan spot size allows us to ensure we obtain a more accurate count of both TROPICS and ERA5 reanalysis data points contained in one scan spot, versus using a constant size across the length of a scan.

5) ERA5 Reanalysis: After all of the TROPICS Pathfinder data points are filtered as described above, we are left with Pathfinder observation points that are restricted to latitudes between 40° N to 40° S, $\pm 10°$ of nadir, over-ocean, and cloud-free. The latitude, longitude, and time of each remaining data point is then matched spatially with the four nearest ERA5 points. We spatially interpolate the four nearest ERA5 data points to calculate the ERA5 values corresponding with the Pathfinder observation location.

This spatial interpolation is performed twice, once for the ERA5 data on the hour before the Pathfinder observation and once for the hour after. The two spatially-interpolated reanalysis points are then temporally interpolated to match the reanalysis data to the Pathfinder observation time. The resulting value is an interpolated reanalysis data point of the weather at the time and location of the TROPICS observation. The interpolated point serves as the input for the CRTM calculations to generate the simulated atmospheric state for the Observed-Simulated data comparison.

C. CRTM Simulation

We use CRTM version 2.3.0 to generate simulated radiances based on the input interpolated ERA5 data, which results in the simulated data for the O-S calculation. CRTM is a one-dimensional radiative transfer model written in Fortran that was designed to perform fast and accurate radiative transfer simulations of Earth's atmosphere. One of its key benefits is that it acts as a satellite simulator [43]. CRTM takes atmospheric profile data, surface data, satellite coefficients, and scan angles as input to calculate simulated brightness temperatures [43].

While this research builds upon previous work utilizing MicroMAS-2A data and ERA5 with the CRTM as the radiative transfer model [7], we also examined suitability of the Radiative Transfer for the TIROS (Television InfraRed Observation Satellite) Operational Vertical Sounder (RTTOV) model for the frequencies and applications of the TROPICS Pathfinder radiometer. CRTM and RTTOV are generally in good agreement with each other, however there are instances where the CRTM performs slightly better than RTTOV, such as near 90 GHz and 183 GHz when compared to ATMS observations [40].

We use sensor coefficients in the CRTM that are specific to TROPICS Pathfinder and were provided by the TROPICS program [44]. These coefficients are projected to be standard in version 2.4.1 of CRTM, which is currently under development.

Using the ERA5 data (see Section II-B5), we generate the atmospheric, surface, and geometry profile files for the filtered TROPICS data points in our MATLAB routine. The atmospheric profile files store atmospheric properties such as temperature, pressure, and absorber quantities. The surface profile files store information about Earth's surface such as type of surface, temperature, and surface type parameters. The geometry profile files store the corresponding scan geometry for each TROPICS observation, including the sensor scan angles and zenith angles. Together, these profiles store information for each TROPICS data point so that the CRTM can simulate the atmospheric conditions at the time of each TROPICS observation. The surface type, atmospheric profile, and absorber definitions used in this work are provided in Table III.

The model used in the CRTM for ocean surface emissivity is the Fast Emissivity Model (FASTEM) [24], [45]–[47]. Land emissivity values are pulled from an atlas for land surface emissivity [24], [48]. Surface types are pulled from files containing different reflectivity schemes, as categorized by the National Polar-orbiting Operational Environmental Satellite System (NPOESS) [24], [42]. Surface type names and values are more thoroughly described in the CRTM v3.1.0 User Guide [42], and the values used in the surface profiles for this work are shown in Table III.

III. RESULTS

We processed all available L1B radiance data (version 1.0) [6] from October 2021 for our analysis. Because this dataset comes from Pathfinder, which is in a sun-synchronous orbit, we limited our analysis to observations between 40° N to 40° S in latitude to be more representative of the full TROPICS constellation's inclinations. We have also filtered the data for observations at longitudes covered by either the GOES-16 or GOES-17 BCMs. This criteria resulted in matchups ranging from 157,131 to 327,900 points. There is a range of matchups for each channel group due to the changing observation footprint size, as shown in Table I. Channels in the same group contain the same number of points. Mean differences, standard deviations, and kurtoses for the O-S of each channel are shown in Tables IV, V, and VI, respectively.

As shown in Table IV, the mean (O-S) departures are <0.5 K over clear sky, over-ocean, and near-nadir, indicating good agreement between the simulated brightness temperatures and the observed data from Pathfinder. The standard deviations and kurtoses also decrease as we filter the observed brightness temperatures, confirming agreement between simulated and observed brightness temperatures and suggesting that Pathfinder data is within the calibration accuracy requirement of 1 K.

Channel 1 O-S values are most significantly influenced by the removal of clouds, reducing the mean difference by approximately 95% and the kurtosis by approximately 98%. This behavior illustrates the sensitivity of Channel 1 to water vapor. By removing clouds from our analysis, we remove the data points most affected by water vapor and reduce the modeling uncertainty in our simulated brightness temperatures.

The results for the mean O-S values for channels in Band 2 were most significantly influenced by filtering the observation angle to near-nadir and removing over-land observations, but there is a significant decrease in standard deviation and kurtosis with additional filtering. The results for Band 3 channels show that the observations are most affected by the presence of clouds, with the exception of Channel 9. Channel 9 shows comparatively little change in mean values between Step 2 and Step 3, but has a significant difference compared to other channels in Band 3 when examining standard deviation and kurtosis. Band 4 is most affected by the removal of observations containing cloud data.

A. O-S Histograms of Data

Ideally, the O-S distribution for each channel will have a low standard deviation and low kurtosis, indicating good agreement between the Pathfinder data and simulated brightness temperatures. The ideal O-S difference would be centered at 0 K, indicating there is no difference between the simulated and observed brightness temperatures. The distribution of O-S values for all channels is shown in Figure 6. Channel-specific histograms of O-S data are shown in Figure 7 for channels 1, 5, 10, and 12.

In Figure 6, each histogram contains O-S data plotted at each filtering step to better illustrate how agreement improves for each channel during the filtering and interpolation processes. Most importantly, and as expected, the combination of all four filtering steps results in the best comparison between observations and simulated data. As each of the filtering and interpolation steps is applied, we see the effects on the O-S calculation in Figure 6. In the histograms, this change is emphasized by the decrease in kurtosis and standard deviation values as the steps are added cumulatively. These results are also depicted in Tables IV, V, and VI.

In Figure 7, O-S histograms of representative channels are shown. While all twelve channels are shown in Figure 6, four channels are selected for illustrative purposes in Figure 7, with one channel selected from each of the four bands for analysis as shown in Table I.

Stepping through the statistics at each filtering step in our analysis method better illustrates the reasoning behind the applied filters. In order to obtain the best estimate of calibration accuracy for Pathfinder observations in this initial study, we aimed to reduce the errors introduced to the simulated brightness temperatures through radiative transfer modeling with the CRTM.

B. O-S Heatmap Plots of Data

Heatmaps of the Pathfinder-observed versus simulated brightness temperatures are given in Figure 8. A black line indicating where the observed brightness temperatures equal the simulated brightness temperatures is overlaid for illustrative purposes of a 0 K O-S difference. In the ideal scenario, these plots will exhibit a 1:1 relationship between the simulated and observed values, indicating a high agreement between the observed and simulated brightness temperatures. From Figure 8, it is evident that the O-S data does follow a linear trend very close to the black 1:1 slope with few outliers.

TABLE IV
THE MEAN VALUES OF THE $O-S$ RESULTS FOR EACH CHANNEL FOLLOWING THE DATA FILTERING STEPS DESCRIBED IN SECTION II-B.

Channel	Step 1 (K)	Step 2 (K)	Step 3 (K)	Step 4 (K)
1	2.95	2.72	0.13	0.11
2	0.14	0.08	-0.35	-0.35
3	-0.62	-0.65	-0.43	-0.43
4	-1.20	-1.21	-0.47	-0.48
5	-0.57	-0.56	0.04	0.03
6	0.23	0.23	0.47	0.45
7	0.20	0.21	0.32	0.31
8	-0.33	-0.33	-0.37	-0.39
9	-0.57	-0.56	-0.50	-0.47
10	-0.42	-0.41	-0.05	-0.03
11	-1.35	-1.34	-0.02	-0.02
12	-2.79	-2.78	-0.09	-0.11

TABLE V
THE STANDARD DEVIATION (σ) OF THE $O-S$ RESULTS FOR EACH CHANNEL AT EACH FILTERING STEP, AS DESCRIBED IN SECTION II-B.

Channel	Step 1 (K)	Step 2 (K)	Step 3 (K)	Step 4 (K)
1	8.1	7.6	3.0	3.0
2	8.1	7.9	2.3	2.3
3	7.3	7.1	1.6	1.6
4	6.8	6.7	1.4	1.4
5	5.9	5.8	1.1	1.1
6	1.6	1.6	1.1	1.1
7	4.9	4.8	1.2	1.2
8	4.5	4.5	1.3	1.3
9	5.9	5.8	1.5	1.5
10	6.6	6.5	1.3	1.3
11	8.6	8.4	1.4	1.4
12	11.1	11.0	2.5	2.5

This article has been accepted for publication in IEEE Journal of Selected Topics in Applied Earth Observations and Remote Sensing. This is the author's version which has not been fully edited and
content may change prior to final publication. Citation information: DOI 10.1109/JSTARS.2024.3518541

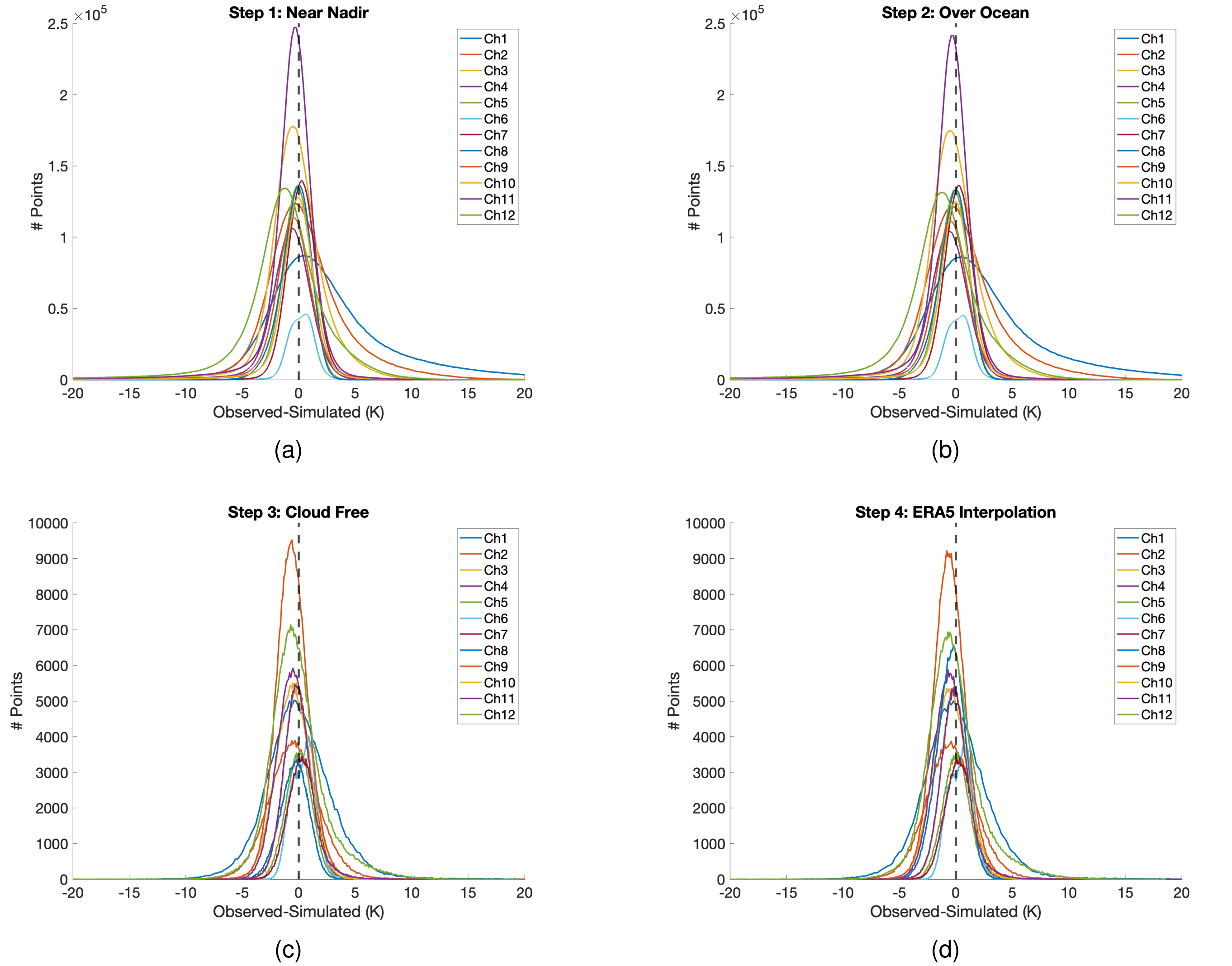

Fig. 6. Histograms of O-S results for each step of the filtering process. Filtering steps are added cumulatively in histograms 6a – 6d. Figure 6a shows the results from filtering for only near-nadir points. Figure 6b shows the results from filtering for only near-nadir and over-ocean. Figure 6c shows the results from filtering for near-nadir, over-ocean, and cloud-free points. Figure 6d shows the results from applying all filters: near-nadir, over-ocean, and cloud-free points and interpolated ERA5 data.

TABLE VI
THE KURTOSIS VALUES OF THE $O - S$ RESULTS FOR EACH CHANNEL AT EACH STEP, AS DESCRIBED IN SECTION II-B

Channel	Step 1 (K)	Step 2 (K)	Step 3 (K)	Step 4 (K)
1	241.9	292.0	7.1	7.1
2	466.0	494.8	4.4	4.4
3	737.2	770.8	3.8	3.8
4	1005.3	1036.2	3.1	3.1
5	1506.8	1542.0	3.0	3.0
6	5989.6	5864.2	3.0	3.0
7	1681.0	1755.4	3.2	3.3
8	1962.6	2000.9	3.1	3.1
9	1357.8	1404.4	9.0	8.9
10	1075.3	1108.0	7.3	7.2
11	478.8	487.4	10.0	9.3
12	107.2	106.2	8.4	8.7

IV. DISCUSSION

The goal of this analysis is to determine the calibration accuracy of the Pathfinder instrument relative to simulated brightness temperatures. To accomplish this, we perform an O-S comparison while limiting errors from other sources, such as the radiative transfer model, CRTM. When we examine the data with the fewest introduced errors in the system (ERA5-induced or modeling-induced errors), we are better able to estimate the calibration accuracy of the observations for an initial validation of the data. If we determine that the observations for clear sky and over-ocean are in good agreement compared to simulated brightness temperatures, we can better infer that all observations are reasonably accurate even if they were not included in this O-S analysis (minus those with observed precipitation). Additionally, no model can capture the full dynamic range of the observations completely, due to errors inherent to radiative transfer modeling.

A. Modeling Induced Error Sources

When performing the O-S comparison, we aim to limit the number of errors introduced by both ERA5 and the CRTM

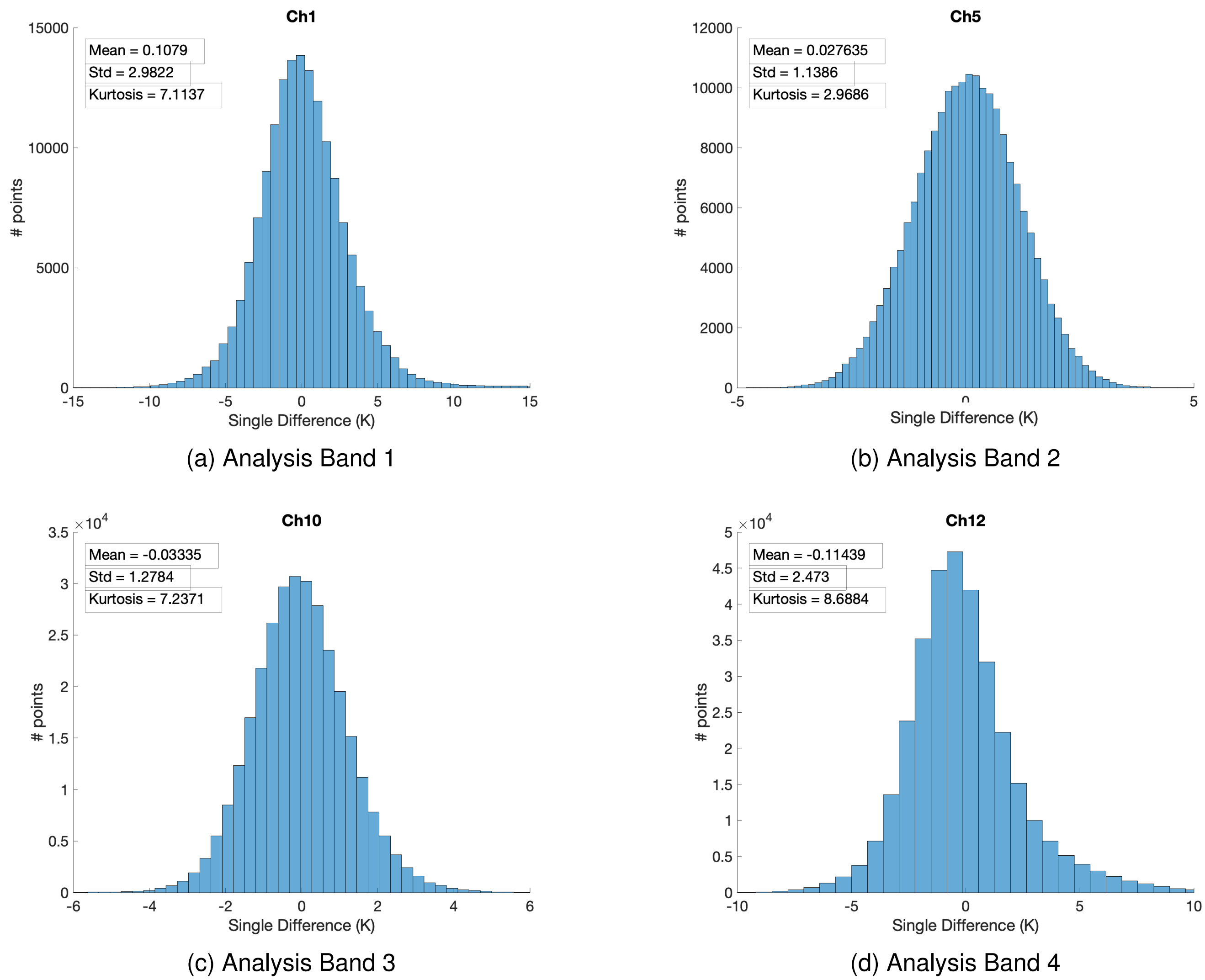

Fig. 7. Histograms of results from October 2021 after the full filtering process. The mean, standard deviation, and kurtosis is shown for channels 1, 5, 10, and 12 in Figures 7a, 7b, 7c, and 7d respectively. These four channels were chosen to represent each of the four analysis bands on Pathfinder, as listed in the last column of Table I.

to the simulated brightness temperatures. Radiative transfer models are subject to errors introduced due to inaccurate spectroscopic databases, atmospheric profiles, surface emissivity, and various assumptions made in the radiative transfer theory. For example, errors in surface emissivity can increase biases of simulations of over land (e.g., [38]). Despite their potential error sources, models like the CRTM are still excellent tools for modeling remote sensing observations.

CRTM is generally very accurate in microwave frequencies over clear sky and over-ocean. Previous work reports the CRTM to be accurate at the level of 0.1 K for frequencies from 10–89 GHz [38]. In regions that are cloudy, accuracy decreases and is on the order of $\sim$5 K, depending on factors such as the frequency of the observation or the cloud type. Accuracy does decrease with increasing frequency, largely due to water vapor continuum absorption effects and increased sensitivity to sources such as thin clouds [38], [40], [49]. This is a region where errors may still arise in our analysis, as the GOES BCM algorithm also has decreased sensitivity to thin clouds, as mentioned in Section II-A2.

ERA5 reanalysis has known uncertainties with precipitation information [35], [36] and observations occurring over land (especially in orographic regions, e.g., [34], see Section II-A3), but has low uncertainties for clear sky and over-ocean regions. By removing TROPICS observations over land, with precipitation events, and with clouds, we are better able to limit non-instrumental errors in our analysis. This is reflected in the results for a majority of channels where the O-S difference decreases with each progressive filtering step, indicating better agreement with additional filtering.

The most improvement occurs with the application of Step 3, which removes cloudy data and focuses only on clear data. This improvement is expected because while each channel is sensitive to different aspects of the atmosphere, each channel is also affected by clouds in different ways, whether it is from scattering of upwelling radiation by cloud particles or the effect of hydrometeors. From this we can conclude that cloud removal is the most important filtering step for analyzing O-S

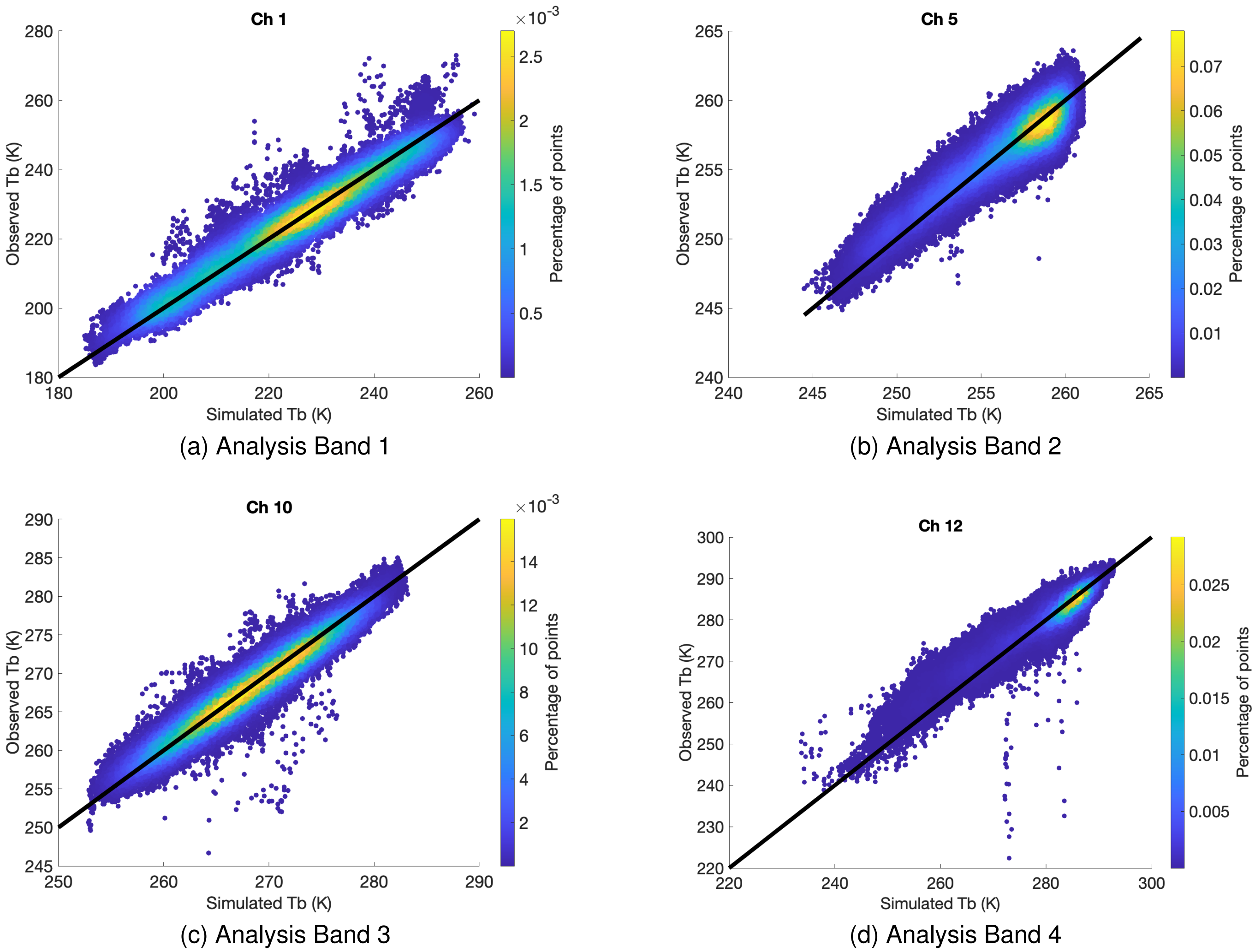

Fig. 8. O-S Pathfinder-observed vs. CRTM-simulated brightness temperature results from October 2021 after all four steps of the filtering process for channels 1, 5, 10, and 12, as shown in Figures 8a, 8b, 8c, and 8d respectively. These four channels were chosen as representative examples each of the four analysis bands on Pathfinder (see Table I).

data overall, followed by filtering observations that are over-ocean. ERA5 reanalysis interpolation also offers improvements in ensuring the input to the simulation is as accurate as possible, albeit at less significant levels.

B. Instrument Error Sources

Instrument error sources can arise from several different sources. As shown in Figures 7 and 8, outliers are extremely uncommon with a substantial percentage of observations showing good agreement with the simulated values. The *calQualityFlag* provided in the TROPICS data products can be applied for future validation as a way to trace the exact source of error for a specific observation.

Based on the results presented in Tables IV, V, and VI and the mission objectives listed in Section I-A, observed brightness temperatures for all twelve Pathfinder channels show good agreement with simulated brightness temperatures. The channels have mean values near 0 (<1 K) and small standard deviations. After applying all four filters, only 1.73% of points in Band 1 are outliers. For Band 2, at most 0.97% of points (Channel 2) are outliers. For Bands 3 and 4, the percentage of outliers ranges from 0.95–1.93% and 3.39%, respectively. We do not remove these outliers from our analysis; all data is included.

The kurtosis values provide a measure of how closely the results resemble a normal distribution and a measure of the outliers. A kurtosis equal to 3 in this case indicates that the data exactly resembles a normal distribution. Random errors with a normal distribution indicate that the radiometer is behaving as expected because it is dominated by thermal (i.e., white) noise. Bands 1, 3, and 4 have increased kurtosis values compared to Band 2. This indicates a slightly larger number of outliers relative to a normal distribution for Bands 1, 3, and 4.

We attribute most of the deviations in O-S results to errors introduced in modeling the simulated brightness temperatures, because the channels with the most outliers are the channels which are most sensitive to water vapor, clouds, and hydrometeors. Only 0.79% of observed points in Channel 12 were labeled as affected by solar or lunar intrusions, as indicated by the data calibration quality flag. Channel 12 would be the channel most affected by intrusions because it has the highest number of points remaining in the analysis due to its small observation footprint (see Table I).

Ultimately, we do not expect outliers to greatly impact mission objectives. The results presented here indicate that Pathfinder radiances fell well within the TROPICS mission requirement of 1 K. Any significant outliers in the full dataset are handled during the calibration process before public data release. The User Guide for TROPICS Data Products describes the thresholds for outliers in detail in section 4.2.7 [23]. For example, unrealistic Earth antenna temperatures (>350 K) are replaced with a filler value by the calibration routine.

V. Conclusion and Future Work

We have presented an initial validation of the TROPICS Pathfinder brightness temperatures by comparing observations to simulated brightness temperatures using ERA5 Reanalysis data and the CRTM. Pathfinder operated for over two years on-orbit and was the first CubeSat sounder to provide global observations of Earth's atmosphere. The O-S results for the TROPICS Pathfinder mission are well within the 1 K minimum mission objectives, as mean values of <0.5 K were validated for observations near-nadir, over-ocean, and clear of clouds during October 2021. We developed a data analysis end-to-end program to use this O-S methodology that will be applied to the full TROPICS constellation and additional Pathfinder data to investigate calibration stability and accuracy over time.

A broader set of observing conditions will be included in future radiance validation work, such as: all cross-track observations rather than only near-nadir, land and ocean observations, and all-weather coverage. A cross-comparison with other radiative transfer models, such as RTTOV, would be useful and will also be explored. Additionally, work will be done to validate the data for the full mission constellation and perform "double-differencing" calculations (see [50], for example). "Double-differencing" will compare on-orbit TROPICS data to observations from other on-orbit satellites. This includes microwave radiometer platforms at similar frequencies, such as the ATMS instruments aboard NOAA-20 and -21, Suomi-NPP, and the other TROPICS constellation satellites. Finally, with the launch and commissioning of GOES-18 and other future GOES satellites, data from these other observatories will be incorporated into this analysis to ensure up-to-date and accurate cloud observations for comparison.

Acknowledgments

The authors thank Dr. Angela Crews for her insight and work to calibrate and validate microwave radiometer data, and Dr. Benjamin Johnson for sharing his expertise in the CRTM. The authors would like to thank the reviewers for their time, attention, and feedback. Their constructive comments helped us to improve the quality of the paper.

The results contain modified Copernicus Climate Change Service information 2020. Neither the European Commission nor ECMWF is responsible for any use that may be made of the Copernicus information or data it contains.

References

[1] W. J. Blackwell, S. Braun, R. Bennartz, C. Velden, M. DeMaria, R. Atlas, J. Dunion, F. Marks, R. Rogers, B. Annane *et al.*, "An overview of the TROPICS NASA Earth Venture mission," *Quarterly Journal of the Royal Meteorological Society*, vol. 144, pp. 16–26, 2018.

[2] L. Ricciardulli, B. Howell, C. R. Jackson, J. Hawkins, J. Courtney, A. Stoffelen, S. Langlade, C. Fogarty, A. Mouche, W. Blackwell, T. Meissner, J. Heming, B. Candy, T. McNally, M. Kazumori, C. Khadke, and M. A. Glaiza Escullar, "Remote sensing and analysis of tropical cyclones: Current and emerging satellite sensors," *Tropical Cyclone Research and Review*, vol. 12, no. 4, pp. 267–293, 2023. [Online]. Available: https://www.sciencedirect.com/science/article/pii/S2225603223000553

[3] Y. You, G. Huffman, C. Kidd, S. Braun, W. Blackwell, J. X. Yang, and C. Da, "Evaluating and improving TROPICS millimeter-wave sounder's precipitation estimate over ocean," *Journal of Geophysical Research: Atmospheres*, vol. 128, no. 16, p. e2023JD038697, 2023, e2023JD038697 2023JD038697. [Online]. Available: https://agupubs.onlinelibrary.wiley.com/doi/abs/10.1029/2023JD038697

[4] C. Kidd, T. Matsui, W. Blackwell, S. Braun, R. Leslie, and Z. Griffith, "Precipitation estimation from the NASA TROPICS mission: Initial retrievals and validation," *Remote Sensing*, vol. 14, no. 13, 2022. [Online]. Available: https://www.mdpi.com/2072-4292/14/13/2992

[5] J. X. Yang, Y.-K. Lee, C. Grassotti, K. Garrett, Q. Liu, W. Blackwell, R. V. Leslie, T. Greenwald, R. Bennartz, and S. Braun, "Atmospheric humidity and temperature sounding from the cubesat TROPICS mission: Early performance evaluation with MiRS," *Remote Sensing of Environment*, vol. 287, p. 113479, 2023. [Online]. Available: https://www.sciencedirect.com/science/article/pii/S0034425723000305

[6] W. J. Blackwell, MIT Lincoln Laboratory, "TROPICS01 Pathfinder L1B Orbital Geolocated Native-Resolution Brightness Temperatures V1.0," Greenbelt, MD, 2023.

[7] A. Crews, W. J. Blackwell, R. V. Leslie, M. Grant, I. A. Osaretin, M. DiLiberto, A. Milstein, S. Leroy, A. Gagnon, and K. Cahoy, "Initial radiance validation of the Microsized Microwave Atmospheric Satellite-2A," *IEEE Transactions on Geoscience and Remote Sensing*, vol. 59, no. 4, pp. 2703–2714, 2021.

[8] W. J. Blackwell, K. E. Clark, J. V. Eshbaugh, and R. V. Leslie, "Qualification of the radiometer suite for the nasa tropics tropical cyclone mission," in *2019 URSI Asia-Pacific Radio Science Conference (AP-RASC)*, 2019, pp. 1–4.

[9] H. W. Christophersen, B. A. Dahl, J. P. Dunion, R. F. Rogers, F. D. Marks, R. Atlas, and W. J. Blackwell, "Impact of TROPICS radiances on tropical cyclone prediction in an OSSE," *Monthly Weather Review*, vol. 149, no. 7, pp. 2279 – 2298, 2021. [Online]. Available: https://journals.ametsoc.org/view/journals/mwre/149/7/MWR-D-20-0339.1.xml

[10] B. C. Technologies, "Blue Canyon Technologies - Documents Library." [Online]. Available: https://bluecanyontech.com/document-library

[11] A. Y. Hou, R. K. Kakar, S. Neeck, A. A. Azarbarzin, C. D. Kummerow, M. Kojima, R. Oki, K. Nakamura, and T. Iguchi, "The global precipitation measurement mission," *Bulletin of the American Meteorological Society*, vol. 95, no. 5, pp. 701 – 722, 2014. [Online]. Available: https://journals.ametsoc.org/view/journals/bams/95/5/bams-d-13-00164.1.xml

[12] S. Gillmer, C. McMenamin, B. Powers, J. Racamato, M. DiLiberto, A. Cunningham, L. Fuhrman, D. Crompton, S. Michael, K. Clark *et al.*, "Precision scanning onboard the nasa tropics mission," in *Proc. ASPE*, 2018.

[13] W. J. Blackwell, A. Cunningham, M. Diliberto, S. Donnelly, J. Eshbaugh, R. V. Leslie, and N. Zorn, "On-orbit results from the NASA TROPICS mission," in *CubeSats and SmallSats for Remote Sensing VI*, vol. 12236. SPIE, 2022, p. 1223602.

[14] L. H. Hoffman, *Calculation and Accuracy of ERBE Scanner Measurement Locations*. National Aeronautics and Space Administration, 1987. [Online]. Available: https://play.google.com/store/books/details?id=24w0jhxzx88C

[15] *TROPICS Level 1 Algorithm Theoretical Basis Document*, National Aeronautics and Space Administration Goddard Earth Science Data Information and Services Center (GES DISC), Goddard, Maryland 20771, 2022.

[16] R. Vincent Leslie, W. J. Blackwell, A. Cunningham, M. DiLiberto, J. Eshbaugh, and I. A. Osaretin, "Pre-launch Calibration of the NASA TROPICS Constellation Mission," in *2020 16th Specialist Meeting on Microwave Radiometry and Remote Sensing for the Environment (MicroRad)*. IEEE, Nov. 2020, pp. 1–4. [Online]. Available: http://dx.doi.org/10.1109/MicroRad49612.2020.9342614

[17] R. V. Leslie, W. J. Blackwell, A. Cunningham, M. DiLiberto, J. Eshbaugh, and I. Osaretin, "Pre-Launch Calibration of the Nasa Tropics Constellation Mission," in *IGARSS 2020 - 2020 IEEE International Geoscience and Remote Sensing Symposium*. Waikoloa, HI, USA: IEEE, Sep. 2020, pp. 6441–6444. [Online]. Available: https://ieeexplore.ieee.org/document/9323744/

[18] R. V. Leslie, W. J. Blackwell, and M. DiLiberto, "Radiometer Calibration for the NASA Tropics Cubesat Mission," in *2021 IEEE International Geoscience and Remote Sensing Symposium IGARSS*. Brussels, Belgium: IEEE, Jul. 2021, pp. 992–995. [Online]. Available: https://ieeexplore.ieee.org/document/9554423/

[19] W. J. Blackwell, D. Crompton, A. Cunningham, S. Donnelly, J. Eshbaugh, V. Leslie, B. Powers, N. Zorn, L. Laboratory, K. Cahoy, A. Gagnon, S. Hasler, D. Adams, O. Hart, J. Johansen, I. Murray, B. Kim, W. McCarty, G. Skrobot, G. Taylor, S. Cooke, M. Grant, and S. Braun, "The NASA Time-Resolved Observations of Precipitation structure and storm Intensity with a Constellation of Smallsats (TROPICS) Mission: Results from the Pathfinder Demonstration and Look Ahead to the Constellation Mission," in *36th Annual Small Satellite Conference*, Utah State University, Logan, UT, Aug. 2022.

[20] World Meteorological Organization, "Observing Systems Capability Analysis and Review Tool | List of all Instruments." [Online]. Available: https://space.oscar.wmo.int/instruments#

[21] ——, "Observing Systems Capability Analysis and Review Tool | Instrument: MWRI-RM." [Online]. Available: https://space.oscar.wmo.int/instruments/view/mwri_rm

[22] ——, "Observing Systems Capability Analysis and Review Tool | Instrument: ATMS." [Online]. Available: https://space.oscar.wmo.int/instruments/view/atms

[23] *User Guide for TROPICS Data Products*, National Aeronautics and Space Administration Goddard Earth Science Data Information and Services Center (GES DISC), Goddard, Maryland 20771, 2021.

[24] B. T. Johnson, C. Dang, P. Stegmann, Q. Liu, I. Moradi, and T. Auligne, "The community radiative transfer model (CRTM): Community-focused collaborative model development accelerating research to operations," *Bulletin of the American Meteorological Society*, vol. 104, no. 10, pp. E1817–E1830, 2023, publisher: American Meteorological Society Section: Bulletin of the American Meteorological Society. [Online]. Available: https://journals.ametsoc.org/view/journals/bams/104/10/BAMS-D-22-0015.1.xml

[25] *GOES-R Series Product Definition and Users' Guide*, U.S. Department of Commerce, National Oceanic and Atmospheric Administration, NOAA Satellite and Information Service, National Aeronautics and Space Administration, P.O. BOX 9800, Melbourne, Florida 32902-9800, 2019.

[26] GOES-R Algorithm Working Group and GOES-R Series Program, "NOAA GOES-R Series Advanced Baseline Imager (ABI) Level 2 Clear Sky Mask (ACM)," 2018.

[27] *GOES-R Series Data Book*, National Aeronautics and Space Administration, GOES-R Series Program Office, Goddard Space Flight Center, Greenbelt, Maryland 20771, 2019.

[28] *Algorithm Theoretical Basis Document: ABI Cloud Mask*, NOAA NESDIS Center for Satellite Applications and Research, College Park, Maryland, USA, 2012.

[29] A. K. Heidinger, M. J. Pavolonis, C. Calvert, J. Hoffman, S. Nebuda, W. Straka III, A. Walther, and S. Wanzong, "Abi cloud products from the goes-r series," in *The GOES-R Series*. Elsevier, 2020, pp. 43–62.

[30] R. Gelaro, W. McCarty, M. J. Suárez, R. Todling, A. Molod, L. Takacs, C. A. Randles, A. Darmenov, M. G. Bosilovich, R. Reichle *et al.*, "The modern-era retrospective analysis for research and applications, version 2 (MERRA-2)," *Journal of climate*, vol. 30, no. 14, pp. 5419–5454, 2017.

[31] S. Saha, S. Moorthi, X. Wu, J. Wang, S. Nadiga, P. Tripp, D. Behringer, Y.-T. Hou, H.-y. Chuang, M. Iredell, M. Ek, J. Meng, R. Yang, M. P. Mendez, H. Van Den Dool, Q. Zhang, W. Wang, M. Chen, and E. Becker, "The NCEP Climate Forecast System Version 2," *Journal of Climate*, vol. 27, no. 6, pp. 2185–2208, Mar. 2014. [Online]. Available: http://journals.ametsoc.org/doi/10.1175/JCLI-D-12-00823.1

[32] H. Hersbach, B. Bell, P. Berrisford, G. Biavati, A. Horányi, J. Muñoz Sabater, J. Nicolas, C. Peubey, R. Radu, I. Rozum, D. Schepers, A. Simmons, C. Soci, D. Dee, and J.-N. Thépaut, "ERA5 hourly data on pressure levels from 1940 to present," *Copernicus Climate Change Service (C3S) Climate Data Store (CDS)*, 2023.

[33] ——, "ERA5 hourly data on single levels from 1940 to present," *Copernicus Climate Change Service (C3S) Climate Data Store (CDS)*, 2023.

[34] H. Hersbach, B. Bell, P. Berrisford, S. Hirahara, A. Horányi, J. Muñoz-Sabater, J. Nicolas, C. Peubey, R. Radu, D. Schepers, A. Simmons, C. Soci, S. Abdalla, X. Abellan, G. Balsamo, P. Bechtold, G. Biavati, J. Bidlot, M. Bonavita, G. De Chiara, P. Dahlgren, D. Dee, M. Diamantakis, R. Dragani, J. Flemming, R. Forbes, M. Fuentes, A. Geer, L. Haimberger, S. Healy, R. J. Hogan, E. Hólm, M. Janisková, S. Keeley, P. Laloyaux, P. Lopez, C. Lupu, G. Radnoti, P. de Rosnay, I. Rozum, F. Vamborg, S. Villaume, and J.-N. Thépaut, "The era5 global reanalysis," *Quarterly Journal of the Royal Meteorological Society*, vol. 146, no. 730, pp. 1999–2049, 2020. [Online]. Available: https://rmets.onlinelibrary.wiley.com/doi/abs/10.1002/qj.3803

[35] Q. Jiang, W. Li, Z. Fan, X. He, W. Sun, S. Chen, J. Wen, J. Gao, and J. Wang, "Evaluation of the era5 reanalysis precipitation dataset over chinese mainland," *Journal of Hydrology*, vol. 595, p. 125660, 2021. [Online]. Available: https://www.sciencedirect.com/science/article/pii/S0022169420311215

[36] B. Hassler and A. Lauer, "Comparison of reanalysis and observational precipitation datasets including era5 and wfde5," *Atmosphere*, vol. 12, no. 11, p. 1462, 2021.

[37] L. Wu, H. Su, X. Zeng, D. J. Posselt, S. Wong, S. Chen, and A. Stoffelen, "Uncertainty of atmospheric winds in three widely used global reanalysis datasets," *Journal of Applied Meteorology and Climatology*, vol. 63, no. 2, pp. 165 – 180, 2024. [Online]. Available: https://journals.ametsoc.org/view/journals/apme/63/2/JAMC-D-22-0198.1.xml

[38] C. Prigent, P. Liang, Y. Tian, F. Aires, J.-L. Moncet, and S. A. Boukabara, "Evaluation of modeled microwave land surface emissivities with satellite-based estimates," *Journal of Geophysical Research: Atmospheres*, vol. 120, no. 7, pp. 2706–2718, 2015. [Online]. Available: https://agupubs.onlinelibrary.wiley.com/doi/abs/10.1002/2014JD021817

[39] I. Moradi, B. Johnson, P. Stegmann, D. Holdaway, G. Heymsfield, R. Gelaro, and W. McCarty, "Developing a radar signal simulator for the community radiative transfer model," *IEEE Trans. Geosci. Remote Sens.*, vol. 61, pp. 1–13, 2023. [Online]. Available: http://dx.doi.org/10.1109/tgrs.2023.3330067

[40] I. Moradi, M. Goldberg, M. Brath, R. Ferraro, S. A. Buehler, R. Saunders, and N. Sun, "Performance of Radiative Transfer Models in the Microwave Region," *Journal of Geophysical Research: Atmospheres*, vol. 125, no. 6, p. e2019JD031831, Mar. 2020. [Online]. Available: https://agupubs.onlinelibrary.wiley.com/doi/10.1029/2019JD031831

[41] (2022) GOES-17 ABI Performance. Geostationary Operational Environmental Satellites - R Series. [Online]. Available: https://www.goes-r.gov/users/GOES-17-ABI-Performance.html

[42] *Joint Center for Satellite Data Assimilation: CRTM v3.1.0 User Guide*, Joint Center for Satellite Data Assimilation, Boulder, CO 80301, 2024.

[43] Y. Han, "JCSDA community radiative transfer model (CRTM): Version 1," *NOAA Technical Report*, 2006.

[44] P. Stegmann and B. Johnson, private communication, 2021.

[45] N. Bormann, A. Geer, and S. English, "Evaluation of the microwave ocean surface emissivity model FASTEM-5 in the IFS," 02/2012 2012. [Online]. Available: https://www.ecmwf.int/node/8303

[46] Q. Liu, F. Weng, and S. J. English, "An improved fast microwave water emissivity model," *IEEE Transactions on Geoscience and Remote Sensing*, vol. 49, no. 4, pp. 1238–1250, 2011.

[47] S. J. English and T. J. Hewison, "Fast generic millimeter-wave emissivity model," in *Microwave Remote Sensing of the Atmosphere and Environment*, T. Hayasaka, D. L. Wu, Y. Jin, and J. Jiang, Eds., vol. 3503, International Society for Optics and Photonics. SPIE, 1998, pp. 288 – 300. [Online]. Available: https://doi.org/10.1117/12.319490

[48] R. L. Vogel, Q. Liu, Y. Han, and F. Weng, "Evaluating a satellite-derived global infrared land surface emissivity data set for use in radiative transfer modeling," *Journal of Geophysical Research: Atmospheres*, vol. 116, no. D8, 2011.

[49] X. Liang, K. Garrett, Q. Liu, E. S. Maddy, K. Ide, and S. Boukabara, "A Deep-Learning-Based Microwave Radiative Transfer Emulator for Data Assimilation and Remote Sensing," *IEEE Journal of Selected Topics in Applied Earth Observations and Remote Sensing*, vol. 15, pp. 8819–8833, 2022, conference Name: IEEE Journal of Selected Topics in Applied Earth Observations and Remote Sensing. [Online]. Available: https://ieeexplore.ieee.org/abstract/document/9909997

[50] W. Berg, S. T. Brown, B. H. Lim, S. C. Reising, Y. Goncharenko, C. D. Kummerow, T. C. Gaier, and S. Padmanabhan, "Calibration and validation of the TEMPEST-D cubesat radiometer," *IEEE Transactions on Geoscience and Remote Sensing*, vol. 59, no. 6, pp. 4904–4914, 2020.

VI. Biography Section

Amelia Gagnon (Student Member, IEEE) received the B.S. degree in electrical engineering from the University of North Dakota, Grand Forks, ND, USA, in 2015, and the M.S. degree from MIT, Cambridge, MA, USA in 2022. She is pursuing the Ph.D. degree with Space Telecommunications, Astronomy, and Radiation (STAR) Laboratory, MIT, Cambridge, MA, USA related to bioastronautics. In between undergrad and graduate school, she worked at Johns Hopkins University Applied Physics Laboratory, Laurel, MD, USA, on systems engineering for the Parker Solar Probe and on electrical engineering design relating to the Europa Clipper.

Samantha N. Hasler received the B.S. degree in Physics from Southeast Missouri State University, Cape Girardeau, MO, USA in 2019. She is currently a member of the Space Telecommunications, Astronomy, and Radiation (STAR) Laboratory at MIT and working toward the Ph.D. degree in Planetary Science with the Department of Earth, Atmospheric and Planetary Sciences at MIT, Cambridge, MA, USA. Her research interests include remote sensing for planetary atmosphere observations.

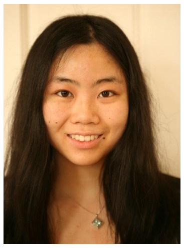

Juliana Chew received the B.S. and M.S. degree in Aerospace Engineering from MIT in 2022 and 2023, respectively. She was a graduate student with the Space Telecommunications, Astronomy, and Radiation (STAR) Laboratory at MIT, focusing on calibration and validation for the NASA TROPICS Pathfinder satellite. She is currently a member of the technical staff at The Aerospace Corporation based in El Segundo, CA.

William J. Blackwell (Fellow, IEEE) received the Sc.D. degree in electrical engineering and computer science from MIT, Cambridge, MA, USA, in 2002.

He is a Laboratory Fellow at MIT Lincoln Laboratory, Lexington, MA and currently serves as the Principal Investigator for the NASA TROPICS Earth Venture mission. His research involves environmental monitoring using ground, air, and space-based sensors.

R. Vincent Leslie (Senior Member, IEEE) received the B.S. degree in electrical engineering from Boston University, Boston, MA, USA, and the M.S. and Ph.D. degrees in electrical engineering from the Massachusetts Institute of Technology (MIT), Cambridge, MA, in 1998, 2000, and 2004, respectively.

He was a Graduate Research Assistant with Remote Sensing and Estimation Group, Research Laboratory of Electronics, MIT, specializing in passive microwave radiometry. He is a member of the Technical Staff with Applied Space Systems Group, MIT Lincoln Laboratory, Lexington, MA, and the TROPICS Instrument Scientist.

Michael DiLiberto received a B.S. degree in electronic engineering technology from Wentworth Institute of Technology, Boston, MA in 2008 and a M.S. degree in electrical engineering from Tufts University, Medford, MA in 2012.

He has been a member of the Technical Staff at MIT Lincoln Laboratory in the Applied Space Systems Group since 2008 and has contributed to a number of remote sensing projects focusing on measuring Earth and its atmosphere. His research interests include radiometer calibration and satellite sensor geolocation.

Kerri Cahoy (Member, IEEE) received the B.S. degree in electrical engineering from Cornell University, Ithaca, NY, USA, in 2000, and the M.S. and Ph.D. degrees in electrical engineering from Stanford University, Stanford, CA, USA, in 2002 and 2008, respectively.

She previously worked at Space Systems Loral, as a Post-Doctoral Fellow at NASA Ames, Mountain View, CA, and currently leads nanosatellite atmospheric sensing, optical communications, and exoplanet technology demonstration missions. She is a Professor and of Aeronautics and Astronautics with MIT, Cambridge, MA, USA, and leads the Space Telecommunications, Astronomy, and Radiation (STAR) Laboratory.